Hindawi
Journal of Sensors
Volume 2021, Article ID 5599025, 13 pages
https://doi.org/10.1155/2021/5599025

Research Article

A Novel Rapid GNSS Network Solution in Mountainous Region Monitoring considering the Tropospheric Delay at Ground Points

Guangwei Jiang,[1,2] **Panlong Wang**,[2] **Bin Wang**,[2] **and Chuanlu Cheng**[2]

[1]*College of Geology Engineering and Geomatics, Chang'an University, 126 Yanta Road, Xi'an 710054, China*
[2]*Geodetic Data Processing Centre of Ministry of Natural Resources, PRC, 334 Youyi Road, Xi'an 710054, China*

Correspondence should be addressed to Guangwei Jiang; 2017026017@chd.edu.cn

Received 7 January 2021; Revised 18 May 2021; Accepted 21 May 2021; Published 3 August 2021

Academic Editor: Sang-Hoon Hong

Due to the short peak observation time of global navigation satellite systems (GNSS), the accuracy of the tropospheric delay estimation and the positioning are poor. In this study, a rapid GNSS network solution for mountainous regions is presented. The high-precision tropospheric delay at ground points is obtained from long-term ground observation data and used as *a priori* constraint in the double-difference equation of short-time synchronous peak observations to realize rapid and high-precision positioning. Chinese mountain survey networks with large elevation gradient (1000~2000 m) were selected for the experimental verification of the proposed method. The results show that the rapid peak positioning method weakened the effect of the residual tropospheric delay caused by the elevation difference, significantly improving the accuracy and reliability of the results. The positioning accuracy of the peak in upward direction was better than 1.1 cm, which meets the requirements of rapid short-span (~1 h) high-precision monitoring and achieves 24 h positioning accuracy. Compared with the traditional solution strategy, the precision of the method with respect to the north (N), east (E), upward (U), and zenith tropospheric delay (ZTD) significantly improved. The accuracy of U improved by more than 47%. Therefore, based on the high accuracy and reliability, information of ground stations can be fully utilized to significantly reduce the peak observation time and the operation costs of surveys in mountain regions.

1. Introduction

Tropospheric delay is a major error that occurs during the processing of global navigation satellite system (GNSS) data. The refined processing of the tropospheric delay correction is the premise of precise and rapid GNSS positioning and is of great significance for rapid and high-precision location services. Due to the complex climatic conditions in high-altitude regions and the lack of measured meteorological data, traditional empirical models are mainly based on atmospheric numerical models and the calculated zenith tropospheric delay (ZTD) exhibits a deviation [1, 2]. Therefore, the GNSS double-difference network solution for peaks requires longer observation times to improve the accuracy of the tropospheric delay estimation and determine the heights of mountains. However, the harsh observation environments at mountain peaks complicate long-term GNSS observations. High elevation gradients result in large differences in the tropospheric delays at both ends of the baseline, which cannot be reduced by traditional double-difference observations to meet the centimeter-level positioning requirements. Reducing the effects of the residual tropospheric delay is of vital importance for the improvement of the accuracy of short-term peak positioning.

Surveying practices showed that the observation time in alpine regions is generally less than 4 h. When short-time GNSS peak observation data are estimated by using the traditional delayed tropospheric estimation method, the results of tropospheric parameter estimation largely deviate. This will affect the ambiguity fixing results, thus leading to a low accuracy and poor reliability of the positioning results, especially in high elevation gradient areas [3, 4]. Therefore, in the case of a high elevation gradient in the regional GNSS observation network, there is a strong correlation between spatial position parameters and tropospheric estimation parameters. The accuracy and reliability of the position results mainly

depend on the spatial and temporal accuracy of the regional tropospheric model [5]. Regarding the accuracy of the tropospheric model, Wang et al. analyzed the applicability of the common tropospheric EGNOS/UNB3m/GPT/GPT2 model in different regions and seasons in China [6]. Jian et al. proposed the integration of a ZTD with an atmospheric numerical model to address the insufficient spatiotemporal resolutions of existing tropospheric models and evaluated the model accuracy [7]. Yibin et al. evaluated the global accuracy of the Global Geodetic Observing System (GGOS) total zenith delay product and applied the corrected GGOS-ZTD product to precise point positioning (PPP) to improve the convergence speed in the height direction [1]. To weaken the effect of the tropospheric delay on the geodetic height in high elevation gradient areas, Di et al. studied the influence of the tropospheric delay estimation strategy on the baseline solution using a baseline with a large height difference. The results showed that the effect of the tropospheric delay estimation on the plane can be neglected, but the impact exceeded the uncertainty limit in the upward direction [8]. Wei studied the influence of the tropospheric delay on short baseline time series with large height differences and showed that the height direction time series exhibit false seasonal signals if the tropospheric delay is not estimated [9]. Kaifeng et al. improved the precision of the postprocessing kinematic (PPK) solution as *a priori* value by using the tropospheric zenith delay obtained from the PPP solution. With the development of multimode and multifrequency GNSS rapid positioning technology, the real-time kinematic (RTK) and PPP technology based on the continuously operating reference station (CORS) network has been developed [10]. Several scholars have proposed the improvement of the accuracy and convergence speed of PPP based on enhanced products of the regional CORS atmosphere [11, 12]. The use of the noncombined PPP method, which is based on real-time atmospheric product enhancement, significantly improves the PPP convergence time [13, 14]. These studies provided a reference for the treatment of the residual convection layer in high-altitude areas.

In most of the existing studies, long-term (>24 h) observation data were obtained for experimental objects with large height differences (~100 m). In actual surveys of mountains, such as the elevation measurement of Mount Qomolangma in China in 2005, the GNSS observation time did not exceed 2 h. There is a lack of data processing strategies for short-time double-difference network solutions in regions with large height differences. The research results show that only the effect of the large height difference of the tropospheric delay on the positioning can be addressed and the applicability of the method has several limitations. Based on the abovementioned considerations, the adoption of long-term ground observation data and the tropospheric delay as *a priori* constraints is proposed in this study to substitute simultaneous solutions in the double-difference observation equation, reduce the unknown estimable parameters of the normal equation, and improve the effect of ambiguity fixing as well as the accuracy of tropospheric delay parameters at peak and point coordinates. To investigate the feasibility and reliability of the method proposed in this paper, network experiments were carried out in different mountainous areas in the east, middle, and south of China to compare and analyze the positioning accuracy and advantages and disadvantages of different tropospheric treatment strategies.

2. Tropospheric Delay in Differential Positioning

During the actual positioning process, the effect of the tropospheric delay is similar to that of the ionospheric delay. The tropospheric delay is caused by the neutral atmosphere below 10 km, and the ionospheric delay is due to the propagation medium at a height of ~400 km [15]. Therefore, the tropospheric delay is more susceptible to climate change. When using the double-difference model for positioning, the effect of the tropospheric delay is generally eliminated or weakened based on parameter estimation [16–18]. Currently, three main methods are used for the correction of the tropospheric delay: (1) direct estimation using an empirical model, such as Saastamoinen based on measured meteorological parameters, and the GPT series and IGGtrop series based on the atmospheric numerical model; (2) parameter estimation in which the tropospheric wet delay is used as a parameter; and (3) the high-precision tropospheric delay is directly obtained from sounding data and regarded to be the true value. When the positioning is based on the double-difference model, the effect of the tropospheric delay is generally eliminated or weakened based on parameter estimation [16–18].

Different positioning technologies can be used to reduce the effect of the tropospheric delay error, but when the baseline distance or the height difference are large, it is difficult to eliminate or weaken the tropospheric delay error. The differential residual tropospheric delay affects the accuracy of the baseline solution and thus the solution of the integer ambiguity [19]. In high-precision GNSS positioning, the tropospheric delay is the largest error, followed by the fixed ambiguity. The tropospheric delay can be generally divided into relative and absolute tropospheric delays [20]. The relative tropospheric delay mainly affects the accuracy of the station height estimate, whereas the absolute tropospheric delay mainly causes the deviation of the baseline scale [21].

2.1. Relative Tropospheric Delay. The relative tropospheric delay is the difference in the tropospheric delay between the base stations at both ends of the baseline. Relative tropospheric delay is one of the key factors affecting the height of a station in alpine surveying scenarios, but it is difficult to correct this error using a model. The height errors can be determined as follows:

$$\Delta h = \frac{\Delta \mathrm{ZPD}}{\sin E_{\min}}, \tag{1}$$

where ΔZPD (zenith path delay) is the relative tropospheric delay and $E_{\min}$ is the cutoff altitude angle of the satellite.

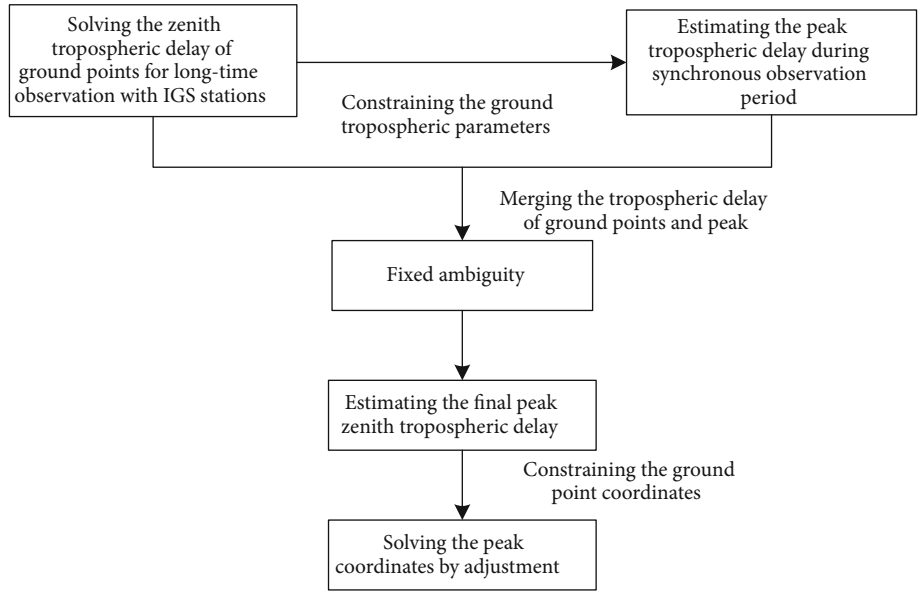

Figure 1: Flowchart of rapid peak positioning based on the *a priori* tropospheric delay at ground points.

Based on Equation (1), the effect of the relative zenith tropospheric delay ΔZTD on the height can be calculated as follows:

$$\Delta h = \frac{\Delta \mathrm{ZPD}}{\sin E_{\min}} = \frac{\Delta \mathrm{ZTD}/\sin E_{\min}}{\sin E_{\min}} = \frac{\Delta \mathrm{ZTD}}{\sin^2 E_{\min}}. \quad (2)$$

Based on this equation, a ZTD of 1 mm causes a height error of 3.5 cm when the cutoff altitude angle of the satellite is 10°. When the cutoff altitude angle of the satellite is 5°, a ZTD of 1 mm causes a height error of 13.2 cm.

2.2. Absolute Tropospheric Delay. The absolute tropospheric delay refers to the same value of tropospheric delay at both ends of the baseline, which mainly affects the scale factor of the baseline. The absolute tropospheric delay can be used to obtain a high-precision zenith delay value by nondifferential precise single-point positioning and a double-difference network solution. The following equation can be used to estimate the scale effect:

$$\frac{\Delta l}{l} = \frac{\mathrm{ZTD}}{R_e \sin E_{\min}}, \quad (3)$$

where l and Δl are the baseline length and deviation, respectively; ZTD is the absolute zenith tropospheric delay, and R_e is the Earth's radius. When the cutoff angle of the satellite altitude is 10°, the scale error caused by an absolute tropospheric delay of 2 m is ~2 ppm. When the cutoff angle of the satellite altitude is 5°, the scale error caused by a 2 m absolute tropospheric delay is ~4 ppm.

3. Double-Difference Function Model considering Delay Constraints in the Troposphere at Ground Points

When the GNSS synchronous observation network is solved with a double-difference baseline, the double-difference equation can be expressed as

$$\begin{cases} P_{1\mathrm{rs}}^{ij} = \rho_{rs}^{ij} + I_{rs}^{ij} + T_{rs}^{ij}, \\ P_{2\mathrm{rs}}^{ij} = \rho_{rs}^{ij} + \dfrac{f_1^2}{f_2^2} I_{rs}^{ij} + T_{rs}^{ij}, \\ \varphi_{1\mathrm{rs}}^{ij} = \rho_{rs}^{ij} - I_{rs}^{ij} + T_{rs}^{ij} + \lambda_1 n_{1rs}^{ij}, \\ \varphi_{2\mathrm{rs}}^{ij} = \rho_{rs}^{ij} - \dfrac{f_1^2}{f_2^2} I_{rs}^{ij} + T_{rs}^{ij} + \lambda_2 n_{2rs}^{ij}. \end{cases} \quad (4)$$

When a nonionospheric combination is used, the double-difference observation equation can be expressed as

$$\begin{cases} \varphi_{\mathrm{IF,rs}}^{ij} = \rho_{rs}^{ij} + \lambda_1 b_{\mathrm{IF,rs}}^{ij} + T_{rs}^{ij}, \\ P_{\mathrm{IF,rs}}^{ij} = \rho_{rs}^{ij} + T_{rs}^{ij}, \end{cases} \quad (5)$$

where the superscripts i and j and the subscripts r and s represent the given receiver and satellite, respectively; ρ_{rs}^{ij} is the geometric distance of the station; I_{rs}^{ij} is the double-difference ionospheric delay; T_{rs}^{ij} is the double-difference tropospheric delay; $\varphi_{\mathrm{IF,rs}}^{ij}$ and $P_{\mathrm{IF,rs}}^{ij}$ are between stations r and s of the observed satellite, which has a nonionospheric combination carrier and pseudorange double-difference observation values; $b_{\mathrm{IF,rs}}^{ij}$ is the double-difference nonionospheric combination ambiguity; and λ_1 is the wavelength at the frequency L_1.

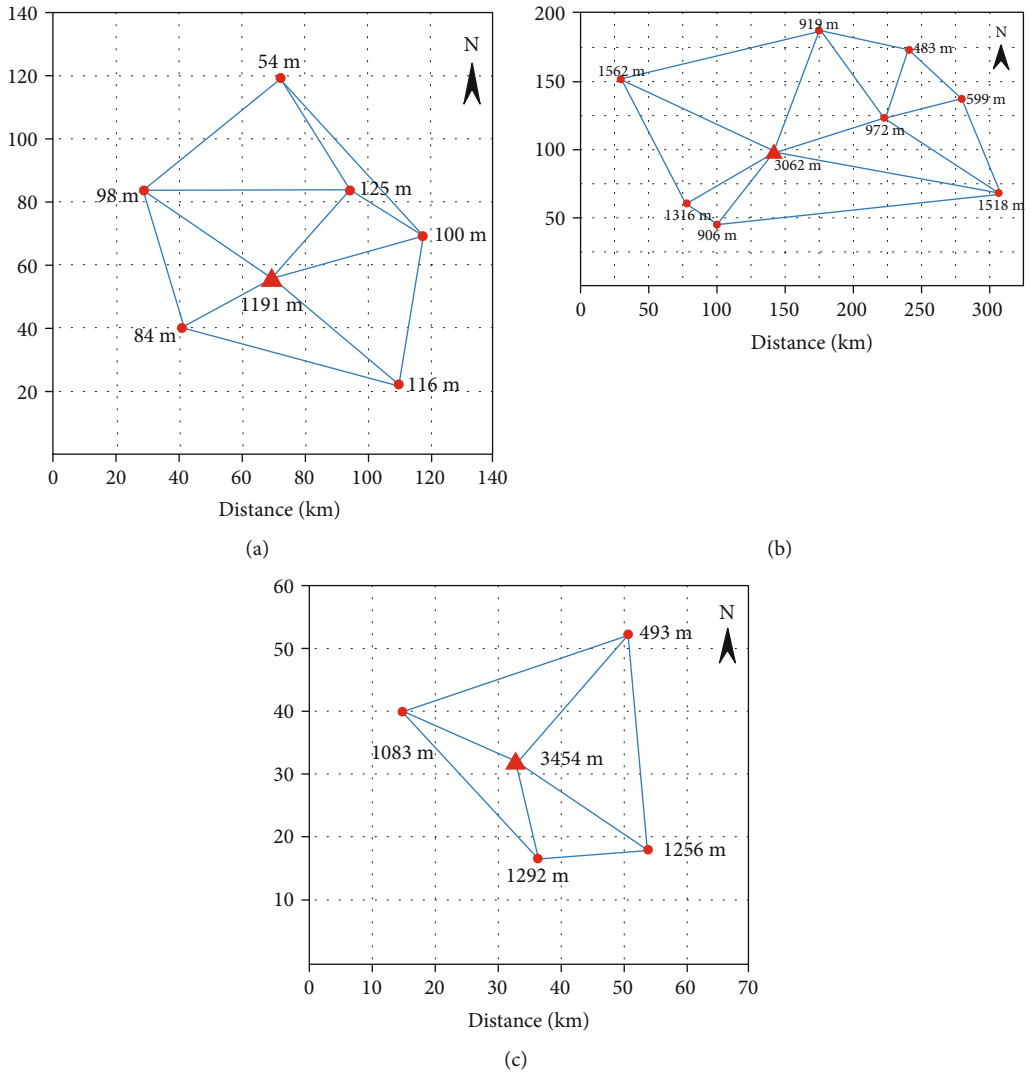

Figure 2: Distribution of the GNSS observation network in different areas. Values next to the red markers indicate elevation. (a) Zhejiang. (b) Yunnan. (c) Shaanxi.

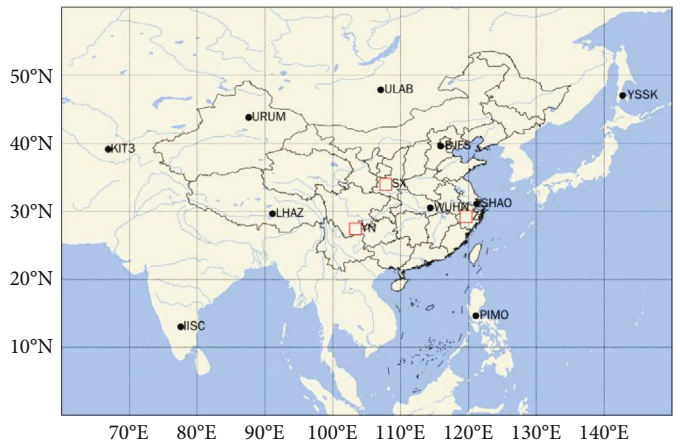

Figure 3: Distribution of IGS stations.

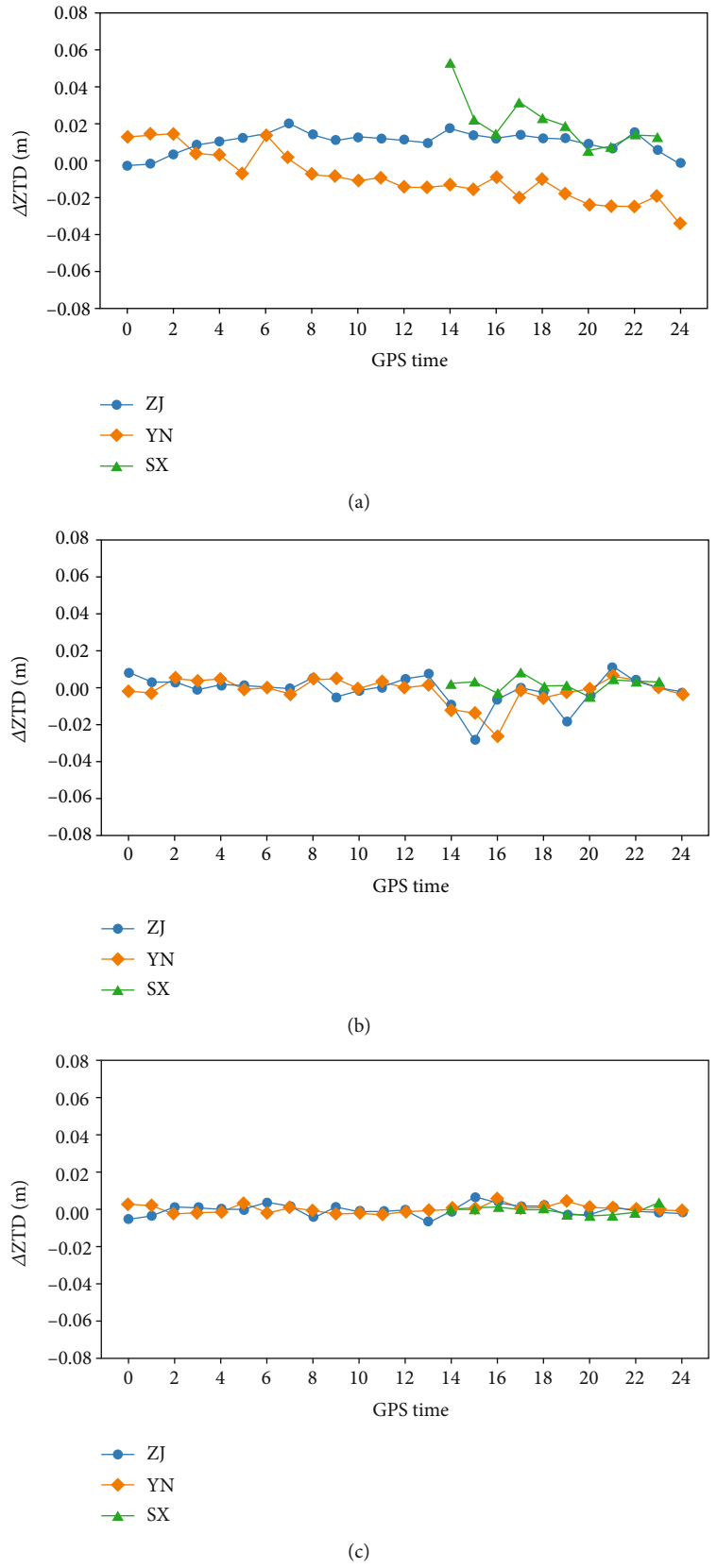

Figure 4: Deviation of the relative zenith tropospheric delay. (a) Scheme 1. (b) Scheme 2. (c) Scheme 3.

Index	N			E			U			ZTD		
	ZJ	YN	SX	ZJ	YN	SX	ZJ	YN	SX	ZJ	YN	SX
MAX	0.017	0.012	0.010	0.043	0.038	0.054	0.054	0.037	0.079	0.019	0.016	0.017
MEAN	0.004	0.002	0.005	0.009	0.005	0.010	0.020	0.019	0.053	0.008	0.006	0.006
RMS	0.006	0.004	0.006	0.016	0.010	0.020	0.025	0.022	0.059	0.007	0.008	0.008

Scheme 1: The Saastamoinen+Vienna mapping functions 1 (VMF1) model value is used for the correction of the tropospheric delay.

Index	N			E			U			ZTD		
	ZJ	YN	SX	ZJ	YN	SX	ZJ	YN	SX	ZJ	YN	SX
MAX	0.018	0.005	0.016	0.053	0.019	0.021	0.049	0.071	0.052	0.361	0.211	0.794
MEAN	0.003	0.002	0.005	0.007	0.005	0.005	0.013	0.014	0.013	0.076	0.056	0.213
RMS	0.005	0.003	0.007	0.015	0.007	0.008	0.018	0.020	0.021	0.118	0.086	0.318

Scheme 2: All stations carry out tropospheric delay estimation. The dry component of the Saastamoinen+Vienna mapping functions 1 (VMF1) model is used as the priori value. The wet component of the tropospheric delay is estimated at all stations. The tropospheric parameters are linearly modelled, so that each period includes the number of the station parameters for the tropospheric delay.

Index	N			E			U			ZTD		
	ZJ	YN	SX	ZJ	YN	SX	ZJ	YN	SX	ZJ	YN	SX
MAX	0.021	0.010	0.006	0.017	0.013	0.006	0.045	0.021	0.018	0.007	0.005	0.004
MEAN	0.002	0.002	0.003	0.003	0.003	0.003	0.013	0.009	0.009	0.002	0.002	0.002
RMS	0.004	0.003	0.003	0.004	0.004	0.004	0.010	0.011	0.010	0.002	0.002	0.002

Scheme 3: The corrections of the tropospheric delay and positioning results obtained from long-term observations of ground points are used as *a priori* constraints, and 1 h sectional solution is obtained for the synchronous peak observation period to estimate the peak tropospheric delay and position of each period.

Based on the assumption of the parameters of the ZTD at the ground points, the stochastic model uses the long-term observed ZTD of the ground points as the virtual observation value and the observation equation can be expressed as

$$\mathrm{VZTD}_r = \mathrm{ZTD}_r + \varepsilon_{r,\mathrm{VZTD}}, \tag{6}$$

where $\varepsilon_{r,\mathrm{VZTD}}$ is the noise of the virtual ZTD. High-precision ground tropospheric delay correction can be achieved due to the ease of long-term GNSS observations in the terrestrial point environment. Equations (5) and (6) can be used to obtain the peak-to-peak tropospheric parameters based on high-precision *a priori* constraints of the troposphere at the ground points.

In this study, the high-precision positioning software BERNESE was used to calculate GNSS observation data at ground points to obtain high-precision positioning results and the tropospheric delay. Based on the use of high-precision *a priori* tropospheric information and ground coordinates as constraints, the double-difference equation can be solved and the number of evaluation parameters can be effectively reduced. The ill-conditioned normal equation can be improved, which enhances the accuracy and reliability of the tropospheric delay, and a peak positioning result is obtained. The solution flowchart is shown in Figure 1.

4. Methods

Surveying practice has shown that a short baseline must consider the effect of tropospheric delay error in high elevation gradient positioning solutions in different regions. In this study, high-precision ground tropospheric correction values were combined with the tropospheric delay of the peak estimation. First, the amount and precision of the tropospheric delay correction calculated from long-tern GNSS observation data for ground points were used as *a priori* constraints in the double-difference observation equation to estimate unknown parameters. Because of the high accuracy of the troposphere parameters solved over a long period of time, as a priori tropospheric constraint, the number of parameters to be determined can be reduced and the morbidity of the normal equation can be improved, thus improving the accuracy and reliability of the tropospheric delay and peak positioning results.

4.1. Experiments in Mountainous Areas. Considering that the GNSS double-difference calculation method is affected by the baseline length and geographical location of the observation network, three mountains in China were selected for experiments to verify the proposed method. The mountains are located in the Zhejiang (ZJ), Yunnan (YN), and Shaanxi (SX) provinces, respectively. The distribution of the stations is shown in Figure 2. The maximum height difference

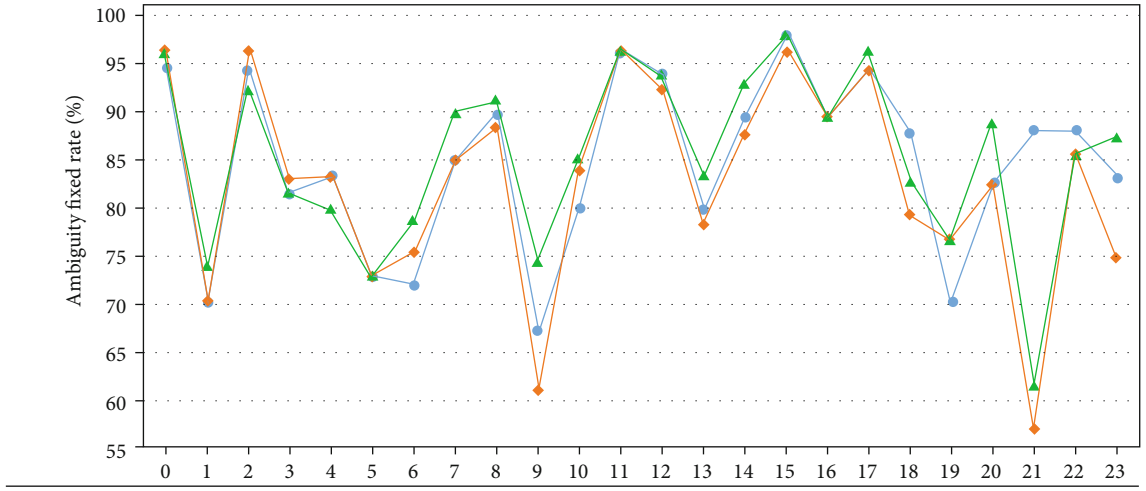

Scheme 1	94.5	70.4	94.4	81.5	83.3	73.1	72.1	85.0	89.9	67.2	80.0	96.4	93.9	80.0	89.5	98.1	89.4	94.4	87.9	70.2	82.6	88.1	88.1	83.3
Scheme 2	96.4	70.4	96.3	83.1	83.3	73.1	75.4	85.0	88.4	61.2	84.0	96.4	92.4	78.3	87.7	96.3	89.4	94.4	79.3	76.6	82.6	57.1	85.7	75.0
Scheme 3	96.4	74.1	92.6	81.5	80.0	73.1	78.7	90.0	91.3	74.6	85.3	96.4	93.9	83.3	93.0	98.1	89.4	96.3	82.8	76.6	89.1	61.9	85.7	87.5

(a)

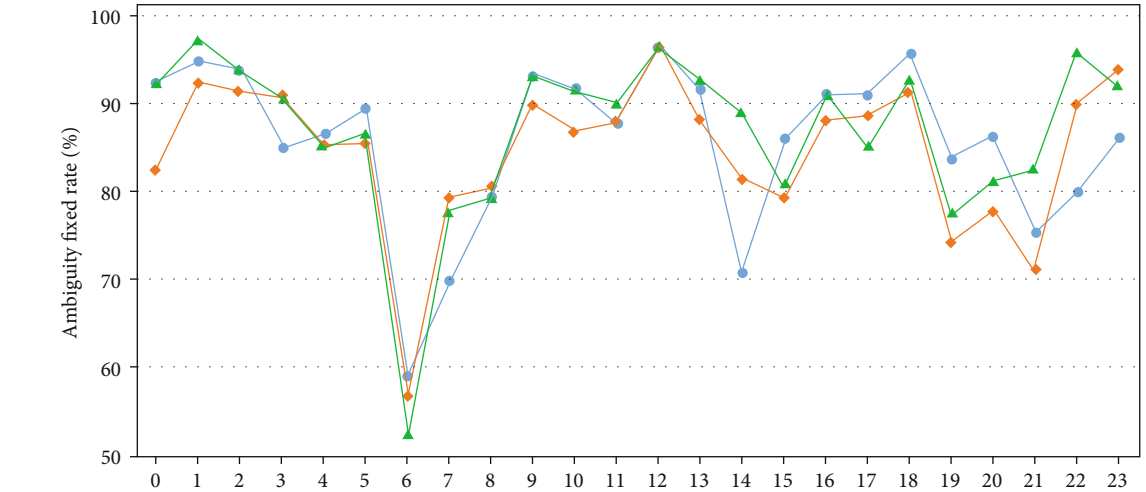

Scheme 1	92.5	95.0	93.9	85.1	86.6	89.5	59.1	69.8	79.3	93.3	91.7	87.9	96.6	91.7	70.8	86.1	91.2	91.2	95.8	83.9	86.4	75.4	80.0	86.3
Scheme 2	82.5	92.5	91.5	90.8	85.4	85.6	56.8	79.4	80.5	90.0	86.9	87.9	96.6	88.1	81.5	79.2	88.2	88.8	91.5	74.2	78.0	71.0	90.0	94.1
Scheme 3	92.5	97.5	93.9	90.8	85.4	86.8	52.3	77.8	79.3	93.3	91.7	90.1	96.6	92.9	89.2	80.6	91.2	85.0	93.0	77.4	81.4	82.6	96.0	92.2

(b)

Figure 5: Continued.

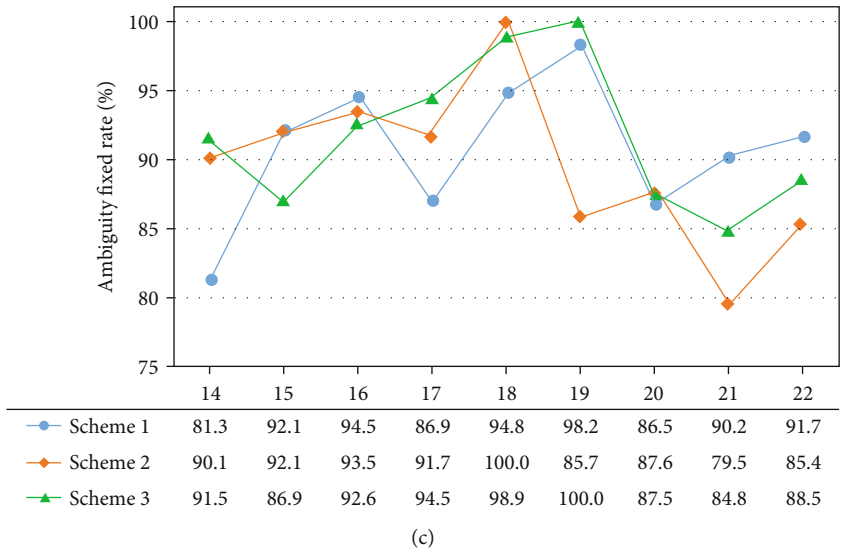

(c)

Figure 5: Success rate of ambiguity fixing: (a) ZJ, (b) YN, and (c) SX.

Table 1: Average ambiguity fixing rate (%).

Mean	ZJ	YN	SX
Scheme 1	84.7	85.8	90.7
Scheme 2	82.8	84.6	89.5
Scheme 3	85.5	87.1	91.7

between the peak and ground point is 1137, 2156, and 2961 m, respectively. Observations were carried out in the Zhejiang and Yunnan provinces for 24 h on March 7 and 1, 2019, respectively. The observation in the Shaanxi Province was carried out on July 31, 2006, for 9 h from 14:00 to 23:00 GPS time. The GNSS dual-frequency receivers were set up between the peak and ground point for continuous observations. The ground points were evenly distributed around the peak. The cutoff angle of the satellite was set to 10°, and the data sampling interval was 30 s.

4.2. Tropospheric Delay Correction and Peak Positioning Results. First, Chinese International GNSS Service (IGS) stations were selected to calculate the ground coordinates under the ITRF2014 framework and the 1 h ZTD using Bernese software. The distribution of the stations is shown in Figure 3. Subsequently, the coordinates of the ground points were used as starting points and positioning results were obtained for the long-term peak observations and ZTD and used as reference values. Finally, the peak data were divided based on 1 h intervals and the results of the short-term mountain network solution were compared and analyzed using the following three tropospheric delay parameter processing schemes.

To obtain a high-precision prior tropospheric delay of ground points, IGS stations around China were used as starting points to calculate the ground coordinates under the ITRF2014 framework and the 1 h ZTD using the Bernese software. The initial tropospheric delay was the dry component of the Saastamoinen model, and the wet component of the tropospheric delay was estimated at a 1 h interval via a piecewise linear method. The tropospheric mapping function adopted VMF1, while the tropospheric delay gradient parameter was not estimated. According to statistics, the ZTD error of ground points was less than 1.2 mm in any period.

To compare the spatiotemporal characteristics of the deviation of the relative ZTD based on the three schemes, three baselines with the largest height differences in different regions were selected and the calculated long-term relative ZTD of the baseline and peak positioning results were used as reference values. The values estimated using the three schemes were compared with the reference values:

$$\begin{cases} \text{bias} = \dfrac{1}{N}\displaystyle\sum_{i=1}^{N}\left(X_i - X_i^{\text{ref}}\right), \\ \text{RMS} = \sqrt{\dfrac{1}{N}\displaystyle\sum_{i=1}^{N}\left(X_i - X_i^{\text{ref}}\right)^2}, \end{cases} \tag{7}$$

where X_i are the positioning and tropospheric zenith delay parameters estimated for each period of different schemes; X_i^{ref} are the reference values for the positioning and tropospheric zenith delay parameters estimated for each period of time; N is the total number of time periods used for the statistics; bias is the average deviation, which reflects the average deviation of different schemes; and RMS is the root mean square error, which reflects the accuracy of different schemes relative to the reference value and the stability of the parameters.

Based on the use of the abovementioned three schemes to locate hilltops with different elevation gradient, the differences between the hilltop positioning results and reference values of the ZTD were compared.

Figure 4 shows that the zenith obtained with Scheme 1 has the largest relative tropospheric delay and a notable

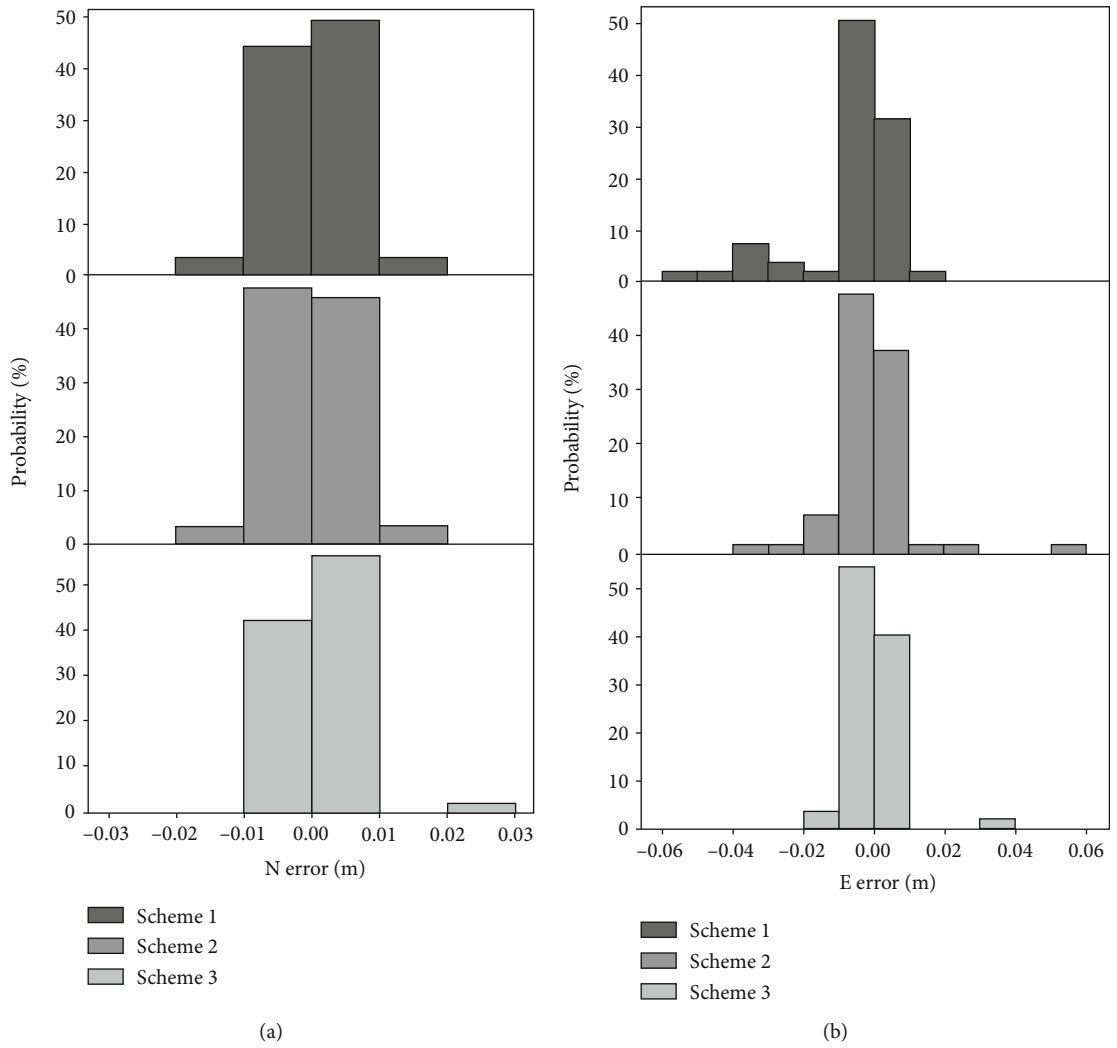

Figure 6: Continued.

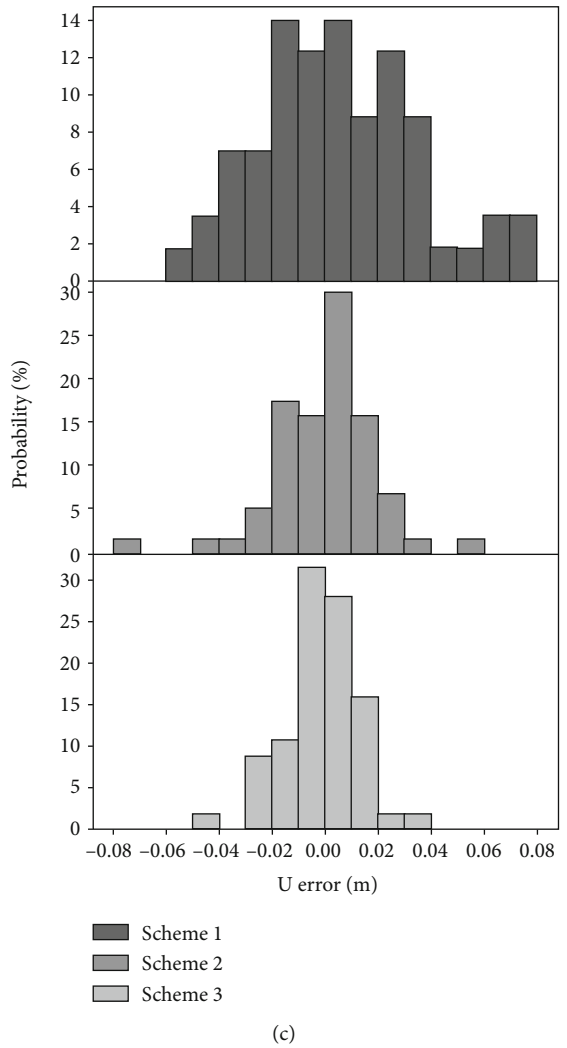

Figure 6: Probability statistics for the positioning error. (a) North. (b) East. (c) Upward.

systematic deviation. The deviation increases with the height difference, and the maximum deviation is 5.38 cm. This indicates that the direct use of the tropospheric model cannot effectively weaken the effect of the tropospheric delay at baselines with high elevation gradient. The zenith troposphere delay based on Scheme 2 is large in several periods, with a maximum deviation of 2.85 cm. On the one hand, uncertainty exists in short-term tropospheric estimations. On the other hand, the correlation between tropospheric parameters and the height difference of the baseline is strong and reliable, and the estimated parameters cannot be correctly calculated in a short time. In Scheme 3, the correlation between the deviation of the zenith relative tropospheric delay and the height difference between the baseline sections is weak. The deviation of the tropospheric delay has the smallest error and the highest stability, and the deviation of the zenith relative troposphere delay is less than 1 cm, which further illustrates that Scheme 3 effectively weakens the effect of the residual tropospheric delay error of baselines with high elevation gradient.

According to the results of the tropospheric delay by the three processing strategies, the baseline ambiguity parameters were fixed. The average success rate of ambiguity fixing was calculated in each period (Figure 5), while the average success rate of ambiguity fixing of all periods is shown in Table 1.

Figure 5 shows that the success rate of ambiguity fixing was influenced by the tropospheric delay, while the impact was small. Comparing the three schemes, the success rate of ambiguity fixing in Scheme 3 was the highest, whereas that in Scheme 2 was the lowest.

The probability statistics for the error of the mountain peak positioning results of the three schemes and the effects of the three schemes on the positioning results were compared. The statistical results are shown in Figure 6.

Figure 6 shows that the error of the planar orientation is smaller than that of the U direction, and the error in the N direction is the smallest. Scheme 1 exhibits the worst stability with respect to the positioning results and has little influence on the positioning results in the N and E directions. The probability of a period with large error is small. The probability of a period with a U direction error below 2 cm is 49.1%, and the reliability of the positioning results is poor. Scheme 2 exhibits a higher stability than Scheme 1 and a

Table 2: Error of the solution and zenith tropospheric delay (m).

(a) Scheme 1

Index	N			E			U			ZTD		
	ZJ	YN	SX	ZJ	YN	SX	ZJ	YN	SX	ZJ	YN	SX
Max	0.017	0.012	0.010	0.043	0.038	0.054	0.054	0.037	0.079	0.019	0.016	0.017
Mean	0.004	0.002	0.005	0.009	0.005	0.010	0.020	0.019	0.053	0.008	0.006	0.006
RMS	0.006	0.004	0.006	0.016	0.010	0.020	0.025	0.022	0.059	0.007	0.008	0.008

(b) Scheme 2

Index	N			E			U			ZTD		
	ZJ	YN	SX	ZJ	YN	SX	ZJ	YN	SX	ZJ	YN	SX
Max	0.018	0.005	0.016	0.053	0.019	0.021	0.049	0.071	0.052	0.361	0.211	0.794
Mean	0.003	0.002	0.005	0.007	0.005	0.005	0.013	0.014	0.013	0.076	0.056	0.213
RMS	0.005	0.003	0.007	0.015	0.007	0.008	0.018	0.020	0.021	0.118	0.086	0.318

(c) Scheme 3

Index	N			E			U			ZTD		
	ZJ	YN	SX	ZJ	YN	SX	ZJ	YN	SX	ZJ	YN	SX
Max	0.021	0.010	0.006	0.017	0.013	0.006	0.045	0.021	0.018	0.007	0.005	0.004
Mean	0.002	0.002	0.003	0.003	0.003	0.003	0.013	0.009	0.009	0.002	0.002	0.002
RMS	0.004	0.003	0.003	0.004	0.004	0.004	0.010	0.011	0.010	0.002	0.002	0.002

Table 3: Statistical results for the average accuracy of the estimated parameters (m).

Index	Mean RMS (m)			Proportion of increase in Scheme 3/%	
Scheme	1	2	3	Compared with Scheme 1	Compared with Scheme 2
N	0.005	0.005	0.003	38	33
E	0.015	0.010	0.004	74	60
U	0.035	0.020	0.010	71	47
ZTD	0.008	0.174	0.002	74	99

larger positioning error. Scheme 3 yields the most stable positioning results. The probability of a large-error period is small, the N direction error of all periods is less than 1 cm, the E direction error in more than 96.4% of the period is less than 1 cm, and the U direction error in more than 86.0% of the period is less than 2 cm.

To further analyze the effects of different schemes on the positioning results, the peak positioning results and errors of the ZTD correction were compared. The statistical results are shown in Table 2.

Based on the statistical tables, the following conclusions can be drawn:

(1) Based on the comparison of Tables 2(a)–2(c), the plane solutions of the three schemes are better than those of the U direction. Scheme 3 exhibits the highest positioning accuracy and reliability, which are less affected by the elevation difference. The average accuracy of N and E is better than 0.4 cm, the accuracy of the U direction is better than 1.1 cm, and the average accuracy is 1.0 cm

(2) Scheme 1 directly reflects the accuracy of the tropospheric delay model. Based on the correction of the tropospheric zenith delay, it can be concluded that the accuracy of the Saastamoinen+VMF1 model reached the mm level in different regions. With increasing height difference, the accuracy of the U direction of the scheme decreases. When the height difference reaches 3000 m, the accuracy of U direction positioning is 5.9 cm, which indicates that the precision of the U direction positioning is 5.9 cm in the high-drop area and the height difference is the main factor affecting the accuracy of height positioning. The tropospheric model contains large errors and delays in the relative troposphere at both ends of the baseline

(3) The estimation of the tropospheric zenith delay parameters based on Scheme 2 exhibits a poor reliability and accuracy. However, the height results are significantly better than those derived from

Scheme 1 because the absolute tropospheric delay error affects the baseline scale and has little influence on the altitude positioning results. The maximum deviation of the positioning results is 1000–2000 m because the relative tropospheric delay error in the corresponding period is large

(4) Based on Scheme 3, the dimension of the observed equation is reduced, and the effective parameters are estimated using *a priori* tropospheric parameters as constraints. The estimated peak-to-peak ZTD accuracy reaches the mm level, which is better than that of Scheme 2. At different elevations in different areas, the average accuracy of elevation positioning is better than 1.0 cm. The weak correlation between the regional height difference and elevation positioning accuracy verifies the validity and reliability of this method. Based on the application of this method, the effect of the altitude difference on the accuracy of elevation positioning is effectively eliminated. Thus, this method is suitable for short-term, high-accuracy, and rapid positioning of GNSS control networks with large height differences

(5) Based on the statistical results obtained for the positioning accuracy of several schemes Table 3, the accuracy of Scheme 3 greatly improved with respect to N, E, U, and ZTD, especially that of U and ZTD. The accuracy in the U direction improved by more than 47%. The accuracies of Scheme 3 are 38%, 74%, 71%, and 74% higher than those in Schemes 1 and 33%, 60%, 47%, and 99% higher than those in Scheme 2. Overall, Scheme 3 is the most suitable for rapid positioning in special environments, such as mountainous areas

5. Conclusions

In this study, the methods and model accuracy of short-term measurements of the tropospheric delay correction with a high elevation gradient were analyzed. In view of the difficulty in estimating the tropospheric delay by using short-term double-difference networks in mountainous areas with large height differences, a high-precision correction of the tropospheric delay based on long-term ground observations is proposed, which can be used as *a priori* constraint and substituted into a double-difference solution model to estimate the peak zenith delay and coordinates. The proposed method was used for an experimental analysis using traditional tropospheric delay estimation and Saastamoinen +VMF1 tropospheric model correction. For both the tropospheric delay and the success rate of ambiguity fixing, the proposed method was most optimal among the three schemes. The results show that the positioning accuracy of this method is better in the N, E, and U directions compared with that of traditional methods. The accuracy in the U direction improved by more than 47%.

In mountainous areas, the rapid GNSS networking method based on tropospheric *a priori* information effectively solves problems regarding the poor stability and positioning accuracy of the geodetic peak height caused by inconsistent tropospheric delays at both ends of the short-term mountain baseline. The accuracy of the positioning results in extreme observation environments improved. This method can be applied to short-term high-accuracy and rapid positioning with large height differences in different areas. In the future, the method must be further improved. The application field should be expanded to realize rapid double-difference positioning based on regional CORS to reduce the peak observation time and to improve the efficiency of positioning operations in mountainous areas.

Data Availability

The datasets used or analyzed during the current study are available from the corresponding author on reasonable request.

Conflicts of Interest

The authors declare no conflict of interest.

Authors' Contributions

Conceptualization was done by G.J. and P.W. Methodology was prepared by P.W. Software was acquired by P.W. Validation was performed by G.J. and P.W. Formal analysis was performed by B.W. and C.C. Resources were acquired by P.W. Supervision was done by G.J. Writing and preparation of original draft was done by G.J. All authors have read and agreed to the published version of the manuscript.

Acknowledgments

This research was funded by the National Natural Science Foundation of China (41574003, 41904040) and the Project for High-level-innovation Talents in Science and Technology, Ministry of Natural Resources (12110600000018003926).

References

[1] Y. Yibin, X. U. Xingyu, and H. Yufeng, "Precision analysis of GGOS tropospheric delay product and its application in PPP," *Acta Geodaetica et Cartographica Sinica*, vol. 46, no. 3, pp. 278–287, 2017.

[2] Y. Xiang, C. Mingjian, W. Jianguang, and C. Rui, "Adaptability analysis of GPT2w model in high latitudes," *Chinese Journal of Space Science*, vol. 40, no. 2, pp. 242–249, 2020.

[3] A. Xiangdong and Y. Dengke, "The impact of the height difference between stations on the baselines solution of short period GPS observations," *Journal of Geodesy and Geodynamics*, vol. 36, no. 6, pp. 534–538, 2016.

[4] Z. Jingyang and S. Shuangshuang, "Research progress of zenith tropospheric delay model and its accuracy analysis over China," *Progress in Geophysics*, vol. 33, no. 1, pp. 148–155, 2018.

[5] J. Junru, T. Tingye, and G. Fei, "A method for increasing precision of short baseline with large height difference by using semi-parametric model," *Journal of Geodesy and Geodynamics*, vol. 36, no. 4, pp. 319–322, 2016.

[6] J. G. Wang, J. P. Chen, J. X. Wang, J. J. Zhang, and L. Song, "Assessment of tropospheric delay correction models over China," *Geomatics and Information Science of Wuhan University*, vol. 41, no. 12, pp. 1656–1663, 2016.

[7] M. Jian, C. Tiejun, L. Xiaoli et al., "A high-accuracy method for tropospheric delay error correction by fusing atmospheric numerical models," *Acta Geodaetica et Cartographica Sinica*, vol. 48, no. 7, pp. 862–870, 2019.

[8] Z. Di, G. Jiming, C. Xuefeng, and Q. Fachao, "Influence of estimation of tropospheric delay on short baseline with big height difference," *Journal of Geodesy and Geodynamic*, vol. 34, no. 2, pp. 146–149, 2014.

[9] W. Wei, "Analysis on influence of tropospheric delay on short baseline time series from GPS stations with the large height difference," *Journal of Geodesy and Geodynamics*, vol. 38, no. 5, pp. 504–509, 2018.

[10] L. Kaifeng, O. Yongzhong, L. Xiuping, and W. Taiqi, "A differential estimation technique of troposphere delay for precise positioning in hydrographic surveying," *Geomatics and Information Science of Wuhan University*, vol. 38, no. 8, pp. 930–934, 2013.

[11] J. Geng, F. N. Teferle, X. Meng, and A. H. Dodson, "Towards PPP-RTK: ambiguity resolution in real-time precise point positioning," *Advances in Space Research*, vol. 47, no. 10, pp. 1664–1673, 2011.

[12] Y. Shoji, "A study of near real-time water vapor analysis using a nationwide dense GPS network of Japan," *Journal of the Meteorological Society of Japan*, vol. 87, no. 1, pp. 1–18, 2009.

[13] Y. Yibin, F. Xinying, P. Wenjie, and L. Lei, "Local atmosphere augmentation based on CORS for real-time PPP," *Geomatics and Information Science of Wuhan University*, vol. 44, no. 12, pp. 1739–1748, 2019.

[14] X. Li, X. Zhang, and M. Ge, "Regional reference network augmented precise point positioning for instantaneous ambiguity resolution," *Journal of Geodesy*, vol. 85, no. 3, pp. 151–158, 2011.

[15] D. Xiaoguang, *Application and Research of Tropospheric Delay Correction in GPS Data Processing*, Chang' an University, 2009.

[16] J. Junru, T. Tingye, and W. Guyue, "A method for increasing precision of single epoch short baseline solution with large height difference by using semi-parametric model," *Science of Surveying and Mapping*, vol. 42, no. 6, pp. 24–30, 2017.

[17] Z. Guoli, Y. Kaiwei, S. Xiaofei, and S. Chuanzhen, "Accuracy impact analysis of tropospheric correction model in double difference RTK solution," *Bulletin of Surveying and Mapping*, vol. 9, pp. 149-150, 2016.

[18] D. Wujiao, C. Zhaohua, and L. Ming, "Effect of height difference on GPS vertical accuracy," *Journal of Geodesy and Geodynamics*, vol. 29, no. 3, pp. 80–83 + 87, 2009.

[19] L. Ning, Z. Yongzhi, and X. Yongliang, "A three-step Kalman filter algorithm for near real-time estimating tropospheric wet delay on GPS reference stations," *Geomatics and Information Science of Wuhan University*, vol. 40, no. 7, pp. 918–923, 2015.

[20] G. Beutler, I. Bauersima, and W. Gurtner, *Atmospheric Refraction and Other Important Biases in GPS Carrier Phase Observations, Monograph12*, School of Surveying, University of New South Wales, 1988.

[21] M. Rothacher and G. Beutler, "The role of GPS in the study of global change," *Physics and Chemistry of the Earth*, vol. 23, no. 9–10, pp. 1029–1040, 1998.